RESEARCH ACTIVITIES X
Okazaki Institute for Integrative Bioscience

X-A Single-Molecule Physiology

A single molecule of protein (or RNA) enzyme acts as a machine which carries out a unique function in cellular activities. To elucidate the mechanisms of various molecular machines, we need to observe closely the behavior of individual molecules, because these machines, unlike man-made machines, operate stochastically and thus cannot be synchronized with each other. By attaching a tag that is huge compared to the size of a molecular machine, or a small tag such as a single fluorophore, we have been able to image the individual behaviors in real time under an optical microscope. Stepping rotation of the central subunit in a single molecule of F_1-ATPase has been videotaped, and now we can discuss its detailed mechanism. RNA polymerase has been shown to be a helical motor that rotates DNA during transcription. Myosin V and VI are also helical motors that move as a left- or right-handed spiral on the right-handed actin helix. Single-molecule physiology is an emerging field of science in which one closely watches individual, 'live' protein/RNA machines at work and examines their responses to external perturbations such as pulling and twisting. I personally believe that molecular machines operate by changing their conformations. Thus, detection of the conformational changes during function is our prime goal. Complementary use of huge and small tags is our major strategy towards this end.

http://www.k2.ims.ac.jp/

X-A-1 One Rotary Mechanism for F_1-ATPase over ATP Concentrations from Millimolar down to Nanomolar

SAKAKI, Naoyoshi; SHIMO-KON, Rieko; ADACHI, Kengo; ITOH, Hiroyasu[1,2]; FURUIKE, Shou; MUNEYUKI, Eiro[3]; YOSHIDA, Masasuke[3,4]; KINOSITA, Kazuhiko, Jr.
([1]Hamamatsu Photonics; [2]CREST; [3]Tokyo Inst. Tech.; [4]ERATO)

[*Biophys. J.* **88**, 2047–2056 (2005)]

F_1-ATPase is a rotary molecular motor in which the central γ-subunit rotates inside a cylinder made of $\alpha_3\beta_3$-subunits. The rotation is driven by ATP hydrolysis in three catalytic sites on the β-subunits. How many of the three catalytic sites are filled with a nucleotide during the course of rotation is an important yet unsettled question. Here we inquire whether F_1 rotates at extremely low ATP concentrations where the site occupancy is expected to be low. We observed under an optical microscope rotation of individual F_1 molecules that carried a bead duplex on the γ-subunit. Time-averaged rotation rate was proportional to the ATP concentration down to 200 pM, giving an apparent rate constant for ATP binding of 2×10^7 $M^{-1}s^{-1}$. A similar rate constant characterized bulk ATP hydrolysis in solution, which obeyed a simple Michaelis-Menten scheme between 6 mM and 60 nM ATP. F_1 produced the same torque of ~40 pN·nm at 2 mM, 60 nM, and 2 nM ATP. These results point to one rotary mechanism governing the entire range of nanomolar to millimolar ATP, although a switchover between two mechanisms cannot be dismissed. Below 1 nM ATP, we observed less regular rotations, indicative of the appearance of another reaction scheme.

X-A-2 ATP-Driven Stepwise Rotation of F_oF_1-ATP Synthase

UENO, Hiroshi[1]; SUZUKI, Toshiharu[1,2]; KINOSITA, Kazuhiko, Jr.; YOSHIDA, Masasuke[1,2]
([1]Tokyo Inst. Tech.; [2]ERATO)

[*Proc. Natl. Acad. Sci. U.S.A.* **102**, 1333–1338 (2005)]

F_oF_1-ATP synthase (F_oF_1) is a motor enzyme that couples ATP synthesis/hydrolysis with a transmembrane proton translocation. F_1, a water-soluble ATPase portion of F_oF_1, rotates by repeating ATP-waiting dwell, 80° substep rotation, catalytic dwell, and 40°-substep rotation. Compared with F_1, rotation of F_oF_1 has yet been poorly understood, and, here, we analyzed ATP-driven rotations of F_oF_1. Rotation was probed with an 80-nm bead attached to the ring of c subunits in the immobilized F_oF_1 and recorded with a submillisecond fast camera. The rotation rates at various ATP concentrations obeyed the curve defined by a K_m of ≈30 μM and a V_{max} of ≈350 revolutions per second (at 37 °C). At low ATP, ATP-waiting dwell was seen and the $k_{on\text{-}ATP}$ was estimated to be 3.6×10^7 $M^{-1}\cdot s^{-1}$. At high ATP, fast, poorly defined stepwise motions were observed that probably reflect the catalytic dwells. When a slowly hydrolyzable substrate, adenosine 5'-[γ-thio]triphosphate, was used, the catalytic dwells consisting of two events were seen more clearly at the angular position of ≈80°. The rotational behavior of F_oF_1 resembles that of F_1. This finding indicates that "friction" in F_o motor is negligible during the ATP-driven rotation. Tributyltin chloride, a specific inhibitor of proton translocation, slowed the rotation rate by 96%. However, dwells at clearly defined angular positions were not observed under these conditions, indicating that inhibition by tributyltin chloride is complex.

X-A-3 Activation of Pausing F_1 Motor by External Force

ONO-HARA, Yoko[1]; ISHIZUKA, Koji[2]; KINOSITA, Kazuhiko, Jr.; YOSHIDA, Masasuke[2];

NOJI, Hiroyuki[1]
([1]Tokyo Inst. Tech.; [2]Univ. Tokyo)

[*Proc. Natl. Acad. Sci. U.S.A.* **102**, 4288–4293 (2005)]

A rotary motor F_1, a catalytic part of ATP synthase, makes a 120° step rotation driven by hydrolysis of one ATP, which consists of 80° and 40° substeps initiated by ATP binding and probably by ADP and/or P_i dissociation, respectively. During active rotations, F_1 spontaneously fails in ADP release and pauses after a 80° substep, which is called the ADP-inhibited form. In the present work, we found that, when pushed >+40° with magnetic tweezers, the pausing F_1 resumes its active rotation after releasing inhibitory ADP. The rate constant of the mechanical activation exponentially increased with the pushed angle, implying that F_1 weakens the affinity of its catalytic site for ADP as the angle goes forward. This finding explains not only its unidirectional nature of rotation, but also its physiological function in ATP synthesis; it would readily bind ADP from solution when rotated backward by an F_o motor in the ATP synthase. Furthermore, the mechanical work for the forced rotation was efficiently converted into work for expelling ADP from the catalytic site, supporting the tight coupling between the rotation and catalytic event.

X-B Bioinorganic Chemistry of Heme-Based Sensor Proteins

Heme-based sensor proteins show a novel function of the heme prosthetic group, in which the heme acts as an active site for sensing the external environmental signal such as diatomic gas molecules and redox change. Heme-based O_2, NO, and CO sensor proteins have now been found in which these gas molecules act as a signaling factor that regulates the functional activity of the sensor proteins. Our research interest focuses on the elucidation of structure-function relationships of CO sensor protein (CooA), O_2 sensor protein (HemAT), and redox sensor protein (DcrA).

X-B-1 Spectroscopic and Redox Properties of a CooA Homologue from *Carboxydothermus hydrogenoformans*

INAGAKI, Sayaka; MASUDA, Chiaki[1]; AKAISHI, Tetsuhiro[1]; NAKAJIMA, Hiroshi; YOSHIOKA, Shiro; OHTA, Takehiro; KITAGAWA, Teizo; AONO, Shigetoshi
([1]JAIST)

[*J. Biol. Chem.* **280**, 3269–3274 (2005)]

CooA is a CO-sensing transcriptional activator that contains a b-type heme as the active site for sensing its physiological effector, CO. In this study, the spectroscopic and redox properties of a new CooA homologue from *Carboxydothermus hydrogenoformans* (Ch-CooA) were studied. Spectroscopic and mutagenesis studies revealed that His-82 and the N-terminal -amino group were the axial ligands of the Fe(III) and Fe(II) hemes in Ch-CooA and that the N-terminal -amino group was replaced by CO upon CO binding. Two neutral ligands, His-82 and the N-terminal -amino group, are coordinated to the Fe(III) heme in Ch-CooA, whereas two negatively charged ligands, a thiolate from Cys-75 and the nitrogen atom of the N-terminal Pro, are the axial ligands of the Fe(III) heme in Rr-CooA. The difference in the coordination structure of the Fe(III) heme resulted in a large positive shift of redox potentials of Ch-CooA compared with Rr-CooA. Comparing the properties of Ch-CooA and Rr-CooA demonstrates that the essential elements for CooA function will be: (i) the heme is six-coordinate in the Fe(III), Fe(II), and Fe(II)–CO forms; (ii) the N-terminal is coordinated to the heme as an axial ligand, and (iii) CO replaces the N-terminal bound to the heme upon CO binding.

X-B-2 Oxygen Sensing Mechanism of HemAT from *B. subtilis*: A Resonance Raman Spectroscopic Study

OHTA, Takehiro; YOSHIMURA, Hideaki; YOSHIOKA, Shiro; AONO, Shigetoshi; KITAGAWA, Teizo

[*J. Am. Chem. Soc.* **126**, 15000–15001 (2004)]

HemAT-Bs is a heme-containing signal transducer protein responsible for aerotaxis of *Bacillus subtilis*, where the heme acts as an oxygen sensor. We have characterized the recombinant *HemAT-Bs* to elucidate the mechanisms of oxygen-sensing and signal transduction by *HemAT-Bs*. *HemAT-Bs* shows similar uv/vis spectra to those of myoglobin (Mb). Site-directed mutagenesis reveals that His123 is the proximal ligand of the heme in *HemAT-Bs*.

Resonance Raman (RR) evidence for structural linkage between the distal side of heme pocket and the signaling domain of an oxygen sensing hemoprotein, *HemAT-Bs*, is reported. The band-fitting analyses of the RR spectra in the Fe–O_2 stretching (ν(Fe–O_2)) region revealed the presence of three conformers with ν(Fe–O_2) at 554, 566, and 572 cm^{-1}, which reflect different H-bond strengths on the bound O_2 molecule. While recent X-ray analysis for CN^--bound *HemAT-Bs* suggested the importance of Thr95 and Tyr70, the species with the strongest H-bond (554 cm^{-1}) was deleted in the T95A mutant and also by removal of the linker and signal domains; however, the Y70F mutant maintained the same three conformers. A scheme for specific O_2 sensing and signaling mechanism is discussed.

X-B-3 Structure and Function of a Novel Redox Sensor DcrA Containing a *C*-Type Heme

YOSHIOKA, Shiro; AONO, Shigetoshi

Chemotaxis signal transducer protein DcrA from a sulfate-reducing bacterium *Desulfovibrio vulgaris* Hildenborough contains a *c*-type heme in its periplasmic domain (DcrA-N), which is the first example of a heme-based sensor protein containing a *c*-type heme as a prosthetic group. Optical absorption and resonance Raman spectroscopy indicates that the heme *c* in DcrA-N shows a redox-dependent ligand exchange. Upon reduction, a water molecule that may be the sixth ligand of the ferric heme *c* is replaced by an endogenous amino acid. Although the reduced heme in DcrA-N is six-coordinated with two endogenous axial ligands, CO can easily bind to the reduced heme to form CO-bound DcrA-N. Reaction of the reduced DcrA-N with molecular oxygen results in autoxidation to form a ferric state without forming any stable oxygen-bound form, probably due to the extremely low redox potential of DcrA-N (–250 mV). DcrA will act as a redox sensor, where the ligand exchange between water and an endogenous amino acid would be a trigger for signal transduction.

X-C Bioinorganic Chemistry of a Novel Heme Enzyme that Catalyzes the Dehydration Reaction

Phenylacetaldoxime dehydratase from *Bacillus* sp. Oxd-1 (OxdB) catalyzes the dehydration reaction of Z-phenylacetaldoxime (PAOx) to produce phenylacetonitrile under mild conditions. OxdB exists in a monomer of a 40-kDa polypeptide containing a protoheme. The heme in OxdB is thought to be the active site for the dehydration reaction. OxdB is the first example of a hemeprotein catalyzing the dehydration reaction physiologically, although many functions of hemeproteins have been elucidated, including oxygen storage/transport, electron transfer, gas molecule sensor, and redox catalysis of various substrates. We are working on OxdB to elucidate the structure-function relationships of this novel heme enzyme.

X-C-1 Regulation of Aldoxime Dehydratase Activity by Redox-Dependent Change in the Coordination Structure of the Aldoxime-Heme Complex

KOBAYASHI, Katsuaki; YOSHIOKA, Shiro; KATO, Yasuo[1]; ASANO, Yasuhisa[1]; AONO, Shigetoshi
([1]Toyama Pref. Univ.)

[*J. Biol. Chem.* **280**, 5486–5490 (2005)]

Phenylacetaldoxime dehydratase from *Bacillus* sp. strain OxB-1 (OxdB) catalyzes the dehydration of Z-phenylacetaldoxime (PAOx) to produce phenylacetonitrile. OxdB contains a protoheme that works as the active center of the dehydration reaction. The enzymatic activity of ferrous OxdB was 1150-fold higher than that of ferric OxdB, indicating that the ferrous heme was the active state in OxdB catalysis. Although ferric OxdB was inactive, the substrate was bound to the ferric heme iron. Electron paramagnetic resonance spectroscopy revealed that the oxygen atom of PAOx was bound to the ferric heme, whereas PAOx was bound to the ferrous heme in OxdB *via* the nitrogen atom of PAOx. These results show a novel mechanism by which the activity of a heme enzyme is regulated; that is, the oxidation state of the heme controls the coordination structure of a substrate-heme complex, which regulates enzymatic activity. Rapid scanning spectroscopy using stopped-flow apparatus revealed that a reaction intermediate (the PAOx-ferrous OxdB complex) showed Soret, α and β bands at 415, 555, and 524 nm, respectively. The formation of this intermediate complex was very fast, finishing within the dead time of the stopped-flow mixer (3 ms). Site-directed mutagenesis revealed that His-306 was the catalytic residue responsible for assisting the elimination of the hydrogen atom of PAOx. The pH dependence of OxdB activity suggested that another amino acid residue that assists the elimination of the OH group of PAOx would work as a catalytic residue along with His-306.

X-D Reaction Mechanism of Metalloenzymes Related to Oxygen Activation

Oxygen is quite important molecule for most organisms. Oxygen is utilized for various physiological functions such as ATP synthesis, defense mechanism, oxidation reactions, and signal transduction. These diverse functions are realized by many metalloenzymes. In this project, we are studying molecular mechanisms of these metalloenzymes.

X-D-1 Oxidizing Intermediates from the Sterically Hindered Salen Iron Complexes Related to the Oxygen Activation by Nonheme Iron Enzymes

KURAHASHI, Takuya; KOBAYASHI, Yoshio[1]; NAGATOMO, Shigenori; TOSHA, Takehiko; KITAGAWA, Teizo; FUJII, Hiroshi
([1]RIKEN)

[*Inorg. Chem.* in press]

Oxidizing intermediates are generated from non-heme iron(III) complexes to investigate the electronic structure and the reactivity, in comparison with the oxoiron(IV) porphyrin π-cation radical (compound I) as a heme enzyme model. Sterically hindered salen iron complexes, bearing a fifth ligand Cl (**1**), OH_2 (**2**), OEt (**3**) and OH (**4**), are oxidized both electrochemically and chemically. Stepwise one-electron oxidation of **1** and **2** generates iron(III)–mono- and diphenoxyl radicals, as revealed by detailed spectroscopic investigations, including UV-Vis, EPR, Mössbauer, resonance Raman, and ESIMS spectroscopies. In contrast to the oxoiron(IV) formation from the hydroxoiron(III) porphyrin upon one-electron oxidation, the hydroxo complex **4** does not generate oxoiron(IV) species. Reaction of **2** with *m*CPBA also results in the formation of the iron (III)–phenoxyl radical. One-electron oxidation of **3** leads to oxidative degradation of the fifth EtO ligand to liberate acetaldehyde even at 203 K. The iron(III)–phenoxyl radical shows high reactivity for alcoxide on iron(III), but exhibits virtually no reactivity for alcohols including even benzyl alcohol without a base to remove an alcohol proton. The present study explains unique properties of mononuclear nonheme enzymes with Tyr residues, and also a poor epoxidation activity of Fe salen compared to Mn and Cr salens.

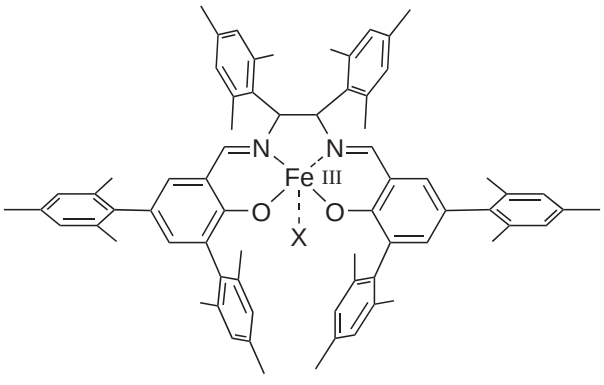

X = Cl (**1**), OH_2 (**2**), OEt (**3**), OH (**4**)

Figure 1. Structure of Sterically Hindered Salen Complexes prepared in this study.

X-D-2 Synthesis of Sterically Hidered Tris(4-imidazolyl)carbinol Ligands and their Copper(I) Complexes Related to Metalloenzymes

KUJIME, Masato; FUJII, Hiroshi

[*Tetrahedron Lett.* **46**, 2809–2812 (2005)]

In non-heme metalloenzymes, imidazole rings of histidine residues often form part of the metal-binding site. For examples, in the active sites of hemocyanin (Cu), nitrite reductase (Cu), and carbonic anhydrase (Zn), three imidazoles coordinate to one metal ion (Figure 1a). Because the coordination environment with three histidine imidazoles are generally occurred in many non-heme metalloenzymes, tripodal N-donor ligands such as hydrotris(2-pyrazolyl)borate and triazacyclononane have been used for synthetic model studies to mimic the active centers. For biomimetic studies, ligands with imidazolyl units are more desirable to understand the nature of metalloenzymes. Especially, a tripodal ligand with three 4-imidazolyl units, *e.g.*, tris(4-imidazolyl)carbinol, is better suited because the coordination enivrionment of this ligand is close to the active sites of metalloenzymes. Therefore, it is desirable the synthesis of tris(4-imidazolyl)carbinol with stable NH protecting group and sterically hidered substituent to mimic the reactive intermediates. Here, we report the synthesis of tris(4-imidazolyl)carbinol ligands having chemically stable methyl group as the NH protective group and bulky substituent (isopropyl or phenyl) for stabilizing reactive species bound to metal center. The copper complexes prepared from these ligands can reproduce the metal active site of copper enzymes and are suitable for biomimetic studies.

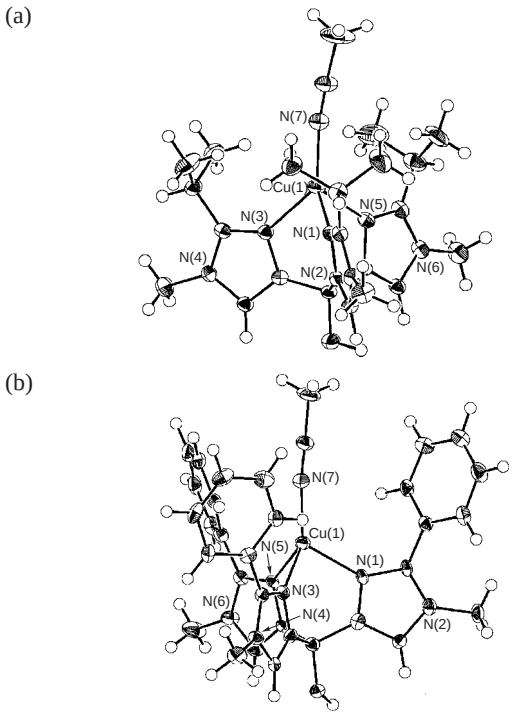

Figure 1. X-ray crystal structures of copper(I) acetonitrile complexes prepared in this study.

X-D-3 O_2- and H_2O_2-Dependent Verdoheme Degradation by Heme Oxygenase: Reaction Mechanisms and Potential Physiological Roles of the Dual Pathway Degradation

MATSUI, Toshitaka[1]; NAKAJIMA, Aya[1]; FUJII, Hiroshi; YOSHIDA, Tadashi[2]; IKEDA-SAITO, Masao[3]
([1]Tohoku Univ.; [2]Yamagata Univ.; [3]IMS and Tohoku Univ.)

[*J. Biol. Chem.* in press]

Heme oxygenase (HO) catalyzes catabolism of heme to biliverdin, CO and a free iron through three successive oxygenation steps. The third oxygenation, oxidative degradation of verdoheme to biliverdin, has been the least understood step in spite of its importance to regulate the HO activity. We have thoroughly examined degradation of a synthetic verdoheme IXa complexed with rat HO-1. Our major findings include: (1) HO degrades verdoheme through a dual pathway using either O_2 or H_2O_2; (2) the newly found H_2O_2 pathway is approximately 40-fold faster than the O_2-dependent degradation; (3) both reactions are initiated by the binding of O_2 or H_2O_2 to allow the first direct observation of degradation intermediates of verdoheme; and (4) Asp140 in HO-1 is critical for the verdoheme degradation regardless of the oxygen source. On the basis of these findings, we propose that the HO enzyme activates O_2 and H_2O_2 on the verdoheme iron with the aid of a nearby water molecule linked with Asp140. These mechanisms are similar to a well-established mechanism of the first oxygenation, *meso*-hydroxylation of heme, and thus, HO can utilize a common architecture to promote the first and third oxygenation steps of the heme catabolism. We also point out a possible involvement of the H_2O_2-dependent verdoheme degradation *in vivo*, and propose potential roles of the dual pathway reaction of HO against oxidative stress.

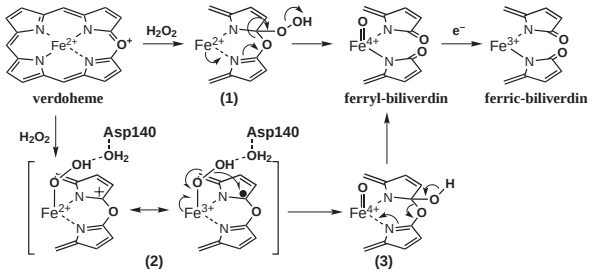

Figure 1. Proposed reaction mechanism of verdoheme in this study.

X-E Reaction Mechanism of Metalloenzymes related to Global Nitrogen Cycle

For all organisms, organic nitrogen and ammonia are required as a constituent part of the cell. In order to keep the environment of the earth constant, the organic nitrogen, fixed nitrogen, must be completely reconverted into dinitrogen gas. The reverse process of the nitrogen fixing is called denitrification process. In this process, nitrate or nitrite ion is reduced to nitrogen gas via nitric oxide and nitrous oxide by many metalloenzymes, nitrate reducatse, nitrite reductase, nitric oxide reductase, and nitrous oxide reductase. In this project, we are studying the molecular mechanism of these metalloenzymes relating to the denitrification process.

X-E-1 Spectroscopic Characterization of Reaction Intermediates in a Model for Copper Nitrite Reductase

KUJIME, Masato; FUJII, Hiroshi

[*Angew. Chem., Int. Ed.* in press]

Reduction of nitrite (NO_2^-) to gaseous nitric oxide (NO) is one of key processes in the global nitrogen cycle and carried out by bacterial copper-containing nitrite reductases (NiR). The enzymes contain two copper ion centers: the type 1 copper site for electron transfer and the type 2 copper site for the catalytic nitrite reduction. Crystallographic and spectroscopic

studies of NiR have proposed the mechanism of the nitrite reduction at the type 2 copper site. The enzyme reaction is initiated by the binding of the nitrite to the reduced form of the type 2 copper site to yield a copper(I) nitrite complex. Subsequently, the copper bound nitrite is reduced to NO and water with intramolecular one electron transfer from the type 2 copper(I) ion and two protons from a conserved aspartic acid placed near the type 2 site. During the course of synthetic study of the copper(I) nitrite complexes, we found that the rapid mixing of copper(I) nitrite complex with trifluoroacetic acid (TFA) with stopped flow at low temperature allows to detect new reaction intermediates in the reduction process. Here, we report detection and characterization of new reaction intermediates in the nitrite reduction. This study shows a new reaction mechanism, in which two protons required for the reaction are not provided to the copper bound nitrite simultaneously but stepwise and that the intramolecular electron transfer from the copper(I) ion to the copper bound nitrite occurs in the second protonation step (Figure 1).

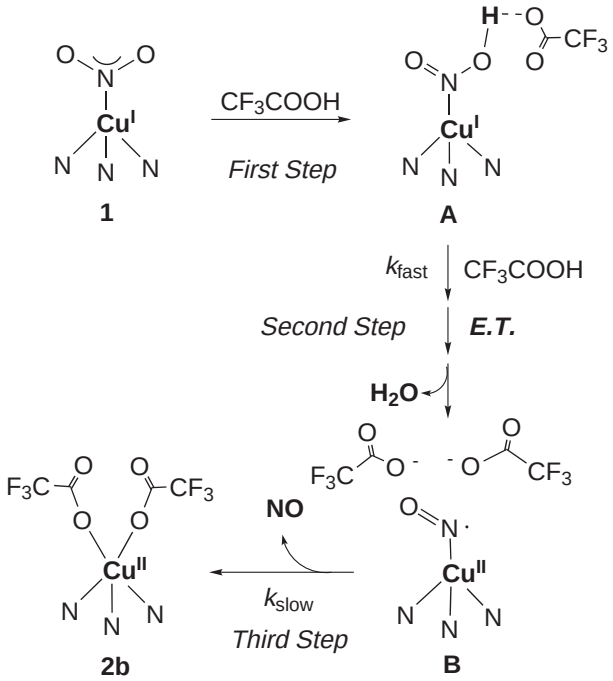

Figure 1. A proposed reaction mechanism of NiR in this study.

X-F Biomolecular Science

Elucidation of a structure-function relationship of metalloproteins and structural chemistry of amyloid fibril are current subjects of this group. The primary technique used for the first project is the stationary and time-resolved resonance Raman spectroscopy excited by visible and UV lasers. Various model compounds of active site of enzymes are also examined with the same technique. IR-microscope dichroism analysis and AFM are the main techniques for the second project. The practical themes that we want to explore for the first project are (1) mechanism of oxygen activation by enzymes, (2) mechanism of active proton translocation and its coupling with electron transfer, (3) structural mechanism of signal sensing and transduction by heme-based sensory proteins, (4) higher order protein structures and their dynamics, and (5) reactions of biological NO. In category (1), we have examined a variety of terminal oxidases, cytochrome P450s (including AOS), and peroxidases, and also treated their reaction intermediates by using the mixed flow transient Raman apparatus and the Raman/absorption simultaneous measurement device. For (2) the third-generation UV resonance Raman (UVRR) spectrometer was constructed and we are applying it to a giant protein like cytochrome *c* oxidase with M_r = 210,000, particularly to explore the oxidation state of Tyr244 in the P_M intermediate. Recently, we succeeded in pursuing protein folding of apomyoglobin by combining the UV time-resolved Raman and rapid mixing techniques. With IR spectroscopy we determined the spectrum of carboxylic side chains of bovine cytochrome oxidase which undergo protonation/deprotonation changes and hydrogen-bonding status changes in response with electron transfers between metal centers or ligand dissociation from heme a_3. In (3) we are interested in a mechanism of ligand recognition specific to CO, NO or O_2 and a communication pathway of the ligand binding information to the functional part of the protein. Several gas sensor heme proteins were extensively treated in this year. For (4) we developed a novel technique for UV resonance Raman measurements based on the combination of the first/second order dispersions of gratings and applied it successfully to 235-nm excited RR spectra of several proteins including mutant hemoglobins and myoglobins. Nowadays we can carry out time-resolved UVRR experiments with nanosecond resolution to discuss protein dynamics. With the system, we have succeeded in isolating the spectrum of tyrosinate in ferric Hb M Iwate, which was protonated in the ferrous state, and the deprotonated state of Tyr244 of bovine cytochrome *c* oxidase. The study is extended to a model of Tyr244, that is, imidazole-bound *para*-cresol coordinated to a metal ion, was synthesized and its UV resonance Raman was investigated. For (5) we purified soluble guanylate cyclase from bovine lung and observed its RR spectra in the presece of allosteric effector, YC-1. The CO and NO adducts in the presence of YC-1 were examined. To further investigate it, we are developing an expression system of this protein. For the amyloid study, we examined FTIR spectra of β_2-microglobulin and its fragment peptides of #11-21, K3, and K3-K7 which form a core part of amyloid fibril of β_2-microglobulin. The effect of seed upon the formation of the fibril was focused this year.

X-F-1 Resonance Raman Characterization of the P Intermediate in the Reaction of Bovine Cytochrome *c* Oxidase

OGURA, Takashi[1]; KITAGAWA, Teizo
([1]IMS and Univ. Hyogo)

[*Biochim. Biophys. Acta* **1655**, 290–297 (2004)]

Reduced cytochrome *c* oxidase binds molecular oxygen, yielding an oxygenated intermediate first (Oxy) and then converts it to water *via* the reaction intermediates of P, F, and O in the order of appearance. We have determined the iron-oxygen stretching frequencies for all the intermediates by using time-resolved resonance Raman spectroscopy. The bound dioxygen in Oxy does not form a bridged structure with Cu_B and the rate of the reaction from Oxy to P (P_R) is slower at higher pH in the pH range between 6.8 and 8.0. It was established that the P intermediate has an oxo-heme and definitely not the Fe_{a3}–O–O–Cu_B peroxy bridged structure. The Fe_{a3}=O stretching frequency ($\nu_{Fe=O}$) of the P_R intermediate, 804/764 cm^{-1} for $^{16}O/^{18}O$, is distinctly higher than that of F intermediate, 785/750 cm^{-1}. The rate of reaction from P to F is quite different between H_2O and D_2O solutions, implicating the coupling of the electron transfer with vector proton transfer in this process. The P intermediate (607 nm form) generated in the reaction of oxidized enzyme with H_2O_2 gave the $\nu_{Fe=O}$ band at 803/769 cm^{-1} and the simultaneously measured absorption spectrum exhibited the difference peak at 607 nm. Reaction of the mixed valence CO adduct with O_2 provided the P intermediate (P_M) giving rise to an absorption peak at 607 nm and the $\nu_{Fe=O}$ bands at 804/768 cm^{-1}. Thus, three kinds of P intermediates are considered to have the same oxo-heme a_3 structure. The ν_4 and ν_2 modes of heme a_3 of the P intermediate were identified at 1377 and 1591 cm^{-1}, respectively, and Raman excitation profiles were different between P and F. These observations may mean the formation of a π cation radical of porphyrin macrocycle in P.

X-F-2 Core Structure of Amyloid Fibril Proposed from IR-Microscope Linear Dichroism

HIRAMATSU, Hirotsugu; GOTO, Yuji[1]; NAIKI, Hironobu[2]; KITAGAWA, Teizo
([1]Osaka Univ.; [2]Fukui Univ.)

[*J. Am. Chem. Soc.* **126**, 3008–3009 (2004)]

A new approach for studying a peptide conformation of amyloid fibril has been developed. It is based on infrared linear dichroism analysis using an IR-microscope for aligned amyloid fibril. The polarization direc-

tions of amide I and II bands were perpendicular similarly for β_2-microglobulin and its #21-31 peptide. Furthermore, this approach has shown that the #21-31 peptide consists of two C=O bonds in the β-sheet that makes 0° with the fibril axis, three C=O bonds in the β-sheet inclined by 27° with respect to the fibril axis, four residues in the random coil by 47°, and two residues in possible β-bulge structure by 32°. Plausible structures of the amyloid core in the fibril are proposed by taking account of these results.

X-F-3 Activation of Heme-Regulated Eukaryotic Initiation Factor 2α Kinase (HRI) Activation by Nitric Oxide Is Induced by the Formation of a Five-Coordinate NO-Heme Complex: Optical Absorption, Electron Spin Resonance and Resonance Raman Spectral Studies

IGARASHI, Jotaro[1]; SATO, Akira[2]; KITAGAWA, Teizo; YOSHIMURA, Tetsuhiko[3]; YAMAUCHI, Seigo[1]; SAGAMI, Ikuko[4]; SHIMIZU, Toru[1]
([1]Tohoku Univ.; [2]SOKENDAI; [3]Inst. Life Support Tec.; [4]Kyoto Pref. Univ.)

[*J. Biol. Chem.* **279**, 15752–15762 (2004)]

Heme-regulated eukaryotic initiation factor 2α kinase (HRI) regulates the synthesis of hemoglobin in reticulocytes in response to heme availability. HRI contains a tightly bound heme at the N-terminal domain. Earlier reports show that nitric oxide (NO) regulates HRI catalysis. However, the mechanism of this process remains unclear. In the present study, we utilize *in vitro* kinase assays, optical absorption, electron spin resonance (ESR), and resonance Raman spectra of purified full-length HRI for the first time to elucidate the regulation mechanism of NO. HRI was activated *via* heme upon NO binding, and the Fe(II)-HRI(NO) complex displayed 5-fold greater eukaryotic initiation factor 2α kinase activity than the Fe(III)-HRI complex. The Fe (III)-HRI complex exhibited a Soret peak at 418 nm and a rhombic ESR signal with g values of 2.49, 2.28, and 1.87, suggesting coordination with Cys as an axial ligand. Interestingly, optical absorption, ESR, and resonance Raman spectra of the Fe(II)-NO complex were characteristic of five-coordinate NO-heme. Spectral findings on the coordination structure of full-length HRI were distinct from those obtained for the isolated N-terminal heme-binding domain. Specifically, six-coordinate NO–Fe(II)–His was observed but not Cys-Fe(III) coordination. It is suggested that significant conformational change(s) in the protein induced by NO binding to the heme lead to HRI activation. We discuss the role of NO and heme in catalysis by HRI, focusing on heme-based sensor proteins.

X-F-4 Steric and Hydrogen-Bonding Effects on the Stability of Copper Complexes with Small Molecules

WADA, Akira[1]; HONDA, Yasutaka[1]; YAMAGUCHI, Syuhei[1]; NAGATOMO, Shigenori; KITAGAWA, Teizo; JITSUKAWA, Koichiro[1]; MASUDA, Hideki[2]
([1]Nagoya Inst. Tech.; [2]IMS and Nagoya Inst. Tech.)

[*Inorg. Chem.* **43**, 5725–5735 (2004)]

A series of the copper(II) complexes with tripodal tetradentate tris(pyridyl 2-methyl)amine-based ligands possessing the hydrogen-bonding 6-aminopyridine units (tapa, three amino groups; bapa, two amino groups; mapa, one amino group) have been synthesized, and their copper(II) complexes with a small molecule such as dioxygen and azide have been studied spectroscopically and structurally. The reaction of their Cu(II) complexes with NaN_3 have given the mononuclear copper complexes with azide in an end-on mode, [Cu(tapa)(N_3)]ClO_4 (**1a**), [Cu(bapa)(N_3)]ClO_4 (**2a**), [Cu(mapa)(N_3)]ClO_4 (**3a**), and [Cu(tpa)(N_3)]ClO_4 (**4a**) (tpa, no amino group). The crystal structures have revealed that the coordination geometries around the metal centers are almost a trigonal-bipyramidal rather than a square-planar except for **1a** with an intermediate between them. The UV-vis and ESR spectral data indicate that the increase of NH_2 groups of ligands causes the structural change from trigonal-bipyramidal to square-pyramidal geometry, which is regulated by a combination of steric repulsion and hydrogen bond. The steric repulsion of amino groups with the azide nitrogen gives rise to elongation of the Cu–N_{py} bonds, which leads to the positive shift of the redox potentials of the complexes. The hydrogen bonds between the coordinated azide and amino nitrogens (2.84–3.05 Å) contribute clearly to the fixation of azide. The Cu(I) complexes with bapa and mapa ligands have been obtained as a precipitate, although that with tapa was not isolated. The reactions of the Cu(I) complexes with dioxygen in MeOH at –75 °C have given the *trans*-μ-1,2 peroxo dinuclear Cu(II) complexes formulated as$[\{(tapa)Cu\}_2(O_2)]^{2+}$ (**1c**), $[\{(bapa)Cu\}_2(O_2)]^{2+}$ (**2c**), and $[\{(mapa)Cu\}_2(O_2)]^{2+}$ (**3c**), whose characterizations were confirmed by UV-vis, ESR, and resonance Raman spectroscopies. UV-vis spectra of **1c**, **2c**, and **3c** exhibited intense bands assignable to $\pi^*(O_2^{2-})$-to-d(Cu) charge transfer (CT) transitions at λ_{max}/nm ($\varepsilon/M^{-1}cm^{-1}$) = 449 (4620), 474 (6860), and 500 (9680), respectively. The series of the peroxo adducts generated was ESR silent. The resonance Raman spectra exhibited the enhanced features assignable to two stretching vibrations $\nu(^{16}O\text{-}^{16}O/^{18}O\text{-}^{18}O)/cm^{-1}$ and $\nu(Cu\text{-}^{16}O/Cu\text{-}^{18}O)/cm^{-1}$ at 853/807 (**1c**), 858/812 (**2c**), 847/800 (**3c**), and at 547/522 (**2c**), 544/518 (**3c**), respectively. The thermal stability of the peroxo-copper species has increased with increase in the number of the hydrogen-bonding interactions between the peroxide and amino groups.

X-F-5 Identification of Crucial Histidines Involved in Carbon-Nitrogen Triple Bond Synthesis by Aldoxime Dehydratase

KONISHI, Kazunobu[1]; ISHIDA, Kyoko[1]; OINUMA, Ken-Ichi[1]; OHTA, Takehiro; HASHIMOTO, Yoshiteru[1]; HIGASHIBATA, Hiroki[1]; KITAGAWA, Teizo; KOBAYASHI, Michihiko[1]
([1]Univ. Tsukuba)

[*J. Biol. Chem.* **279**, 47619–47625 (2004)]

Aldoxime dehydratase (OxdA), which is a novel heme protein, catalyzes the dehydration of an aldoxime to a nitrile even in the presence of water in the reaction mixture. The combination of site-directed mutagenesis of OxdA (mutation of all conserved histidines in the aldoxime dehydratase superfamily), estimation of the heme contents and specific activities of the mutants, and CD and resonance Raman spectroscopic analyses led to the identification of the proximal and distal histidines in this unique enzyme. The heme contents and CD spectra in the far-UV region of all mutants except for the H299A one were almost identical to those of the wild-type OxdA, whereas the H299A mutant lost the ability of binding heme, demonstrating that His^{299} is the proximal histidine. On the other hand, substitution of alanine for His^{320} did not affect the overall structure of OxdA but caused loss of its ability of carbon-nitrogen triple bond synthesis and a lower shift of the Fe–C stretching band in the resonance Raman spectrum for the CO-bound form. Furthermore, the pH dependence of the wild-type OxdA closely followed the His protonation curves observed for other proteins. These findings suggest that His^{320} is located in the distal heme pocket of OxdA and would donate a proton to the substrate in the aldoxime dehydration mechanism.

X-F-6 Thermal Stability of Mononuclear Hydroperoxocopper(II) Species. Effects of Hydrogen Bonding and Hydrophobic Field

YAMAGUCHI, Syuhei[1]; WADA, Akira[1]; NAGATOMO, Shigenori; KITAGAWA, Teizo; JITSUKAWA, Koichiro[1]; MASUDA, Hideki[2]
([1]Nagoya Inst. Tech.; [2]IMS and Nagoya Inst. Tech.)

[*Chem. Lett.* **33**, 1556–1557 (2004)]

The effects of hydrogen bonding and hydrophobic field on the thermal stabilities of Cu(II)–OOH complexes have been studied using tripodal tetradentate ligands with their functional groups on the basis of UV-vis, ESR, ESI-mass, and resonance Raman spectroscopies.

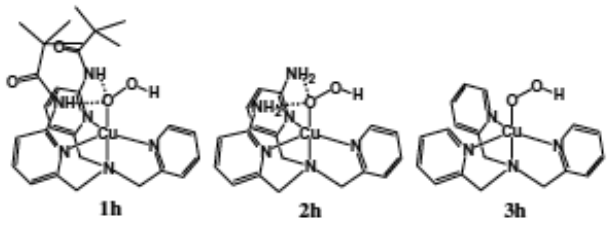

Scheme 1.

We succeeded in obtaining a stable hydroperoxocopper(II) complex with a tripodal tetradentate ligand, bis(6-pivalamido-2-pyridylmethyl)(2-pyridylmethyl)-amine (BPPA) (**1h**)[5] for whhick the crystal structure and spectroscopic characterization of the hydroperoxocopper(II) complex were provided. Raman spectrum of **2h** in acetonitrile measured at –40 °C (using 406.7 nm laser excitation) gave a resonance-enhanced Raman band at 850 cm^{-1}, which shifted to 801 cm^{-1} ($\Delta\nu$ = 49 cm^{-1}) when ^{18}O-labeled H_2O_2 was used. That of **2h** in methanol measured at –80 °C (using 406.7 nm laser excitation) gave Raman bands at 854 and 492 cm^{-1}, assignable to ν(O–O) and ν(Cu–O), respectively. The formation of **2h** was also confirmed from ESI mass spectrum measured in acetonitrile at –20 °C.The resonance Raman spectra of methanol solution of **3h** measured at –80 °C (using 406.7 nm laser excitation) showed a resonance-enhanced Raman band at 847 and 512 cm^{-1}, which are assigned to ν(O–O) and ν(Cu–O), the former of which shifted to 792 cm^{-1} ($\Delta\nu$ = 55 cm^{-1}) when ^{18}O-labeled H_2O_2 was employed. The formation of **3h** was also confirmed from ESI mass spectrum measured in acetonitrile at –40 °C. Interestingly, the effects of hydrogen bonding and hydrophobic field on the thermal stabilities of Cu–OOH species, when their decomposition rates were followed using decrease in the absorption intensities of LMCT bands, was dramatically found out in the stability of these hydroperoxocopper(II) complexes.

X-F-7 Energy Funneling of IR Photons Captured by Dendritic Antennae and Acceptor Mode Specificity: Anti-Stokes Resonance Raman Studies on Iron(III) Porphyrin Complexes with a Poly(Aryl Ether) Dendrimer Framework

MO, Yu-Jun[1]; JIANG, Donglin[2]; UYEMURA, Makoto[2]; AIDA, Takuzo[2]; KITAGAWA, Teizo
([1]IMS and Henan Univ.; [2]Univ. Tokyo)

[*J. Am. Chem. Soc.* **127**, 10020–10027 (2005)]

A series of poly(aryl ether) dendrimer chloro-iron (III)porphyrin complexes (L_nTPP)Fe(III)Cl (number of aryl layers [n] = 3 to 5) were synthesized and their Boltzman temperatures under IR irradiation were evaluated from ratios of Stokes to anti-Stokes intensities of resonance Raman bands. While the Boltzman temperature of neat solvent was unaltered by IR irradiation, (L_nTPP)Fe(III)Cl (n = 3–5) all showed a temperature rise that was larger than that of the solvent and greater as the dendrimer framework was larger. Among vibrational modes of the metalloporphyrin core, the temperature rise of an axial Fe–Cl stretching mode at 355 cm^{-1} was larger than that for a porphyrin in–plane mode at 390 cm^{-1}. Although the most of IR energy is captured by the phenyl ν_8 mode at 1597 cm^{-1} of the dendrimer framework, an anti-Stokes Raman band of the phenyl ν_8 mode was not detected, suggesting the extremely fast vibrational relaxation of the phenyl mode. From these observations, it is proposed that the energy of IR photons captured by the aryl dendrimer framework is transferred to the axial Fe–Cl bond of ironporphyrin core and then relaxed to the porphyrin macrocycle.

X-F-8 Structural Model of the Amyloid Fibril Formed by β_2-Microglobulin #21-31 Fragment Based on Vibrational Spectroscopy

HIRAMATSU, Hirotsugu; GOTO, Yuji[1]; NAIKI, Hironobu[2]; KITAGAWA, Teizo
([1]Osaka Univ.; [2]Fukui Univ.)

[*J. Am. Chem. Soc.* **127**, 7988–7989 (2005)]

A structural model of amyloid fibril formed by the #21-31 fragment of β_2-microglobulin is proposed from microscope IR measurements on specifically ^{13}C-labeled peptide fibrils and Raman spectra of the dispersed fibril solution. The ^{13}C-shifted amide frequency indicated the secondary structure of the labeled residues. The IR spectra have demonstrated that the region between F22 and V27 forms the core part with the extended β-sheet structure. Raman spectra indicated the formation of a dimer with a disulfide bridge between C25 residues.

X-F-9 Excited State Property of Hardly Photodissociable Heme-CO Adduct Studied by Time-Dependent Density Functional Theory

OHTA, Takehiro; PAL, Biswajit; KITAGAWA, Teizo

[*J. Phys. Chem.* in press]

While most of CO-bound hemes are easily photodissociated with a quantum yield of nearly unity, we occasionally encounter a CO-heme which appears hardly photodissociable under ordinary measurement conditions of resonance Raman spectra using CW laser excitation and a spinning cell. This study aims to understand such hemes theoretically, that is, the excited state properties of the five-coordinate heme-CO adduct (5cH) as well as the 6c heme-CO adduct (6cH) with a weak axial ligand. Using a hybrid density functional theory we scrutinized the properties of the ground and excited spin states of the computational models of a 5cH and a water ligated 6cH (6cH-H_2O), and compared these properties with those of a photodissociable imidazole ligated 6cH (6cH-Im). Jahn-Teller softening for the Fe– C–O bending potential in the a_1-e excited state was suggested. The excited state properties of 6cH-Im and 5cH were further studied with time-dependent DFT theory. The reaction products of the 6cH-Im and 5cH were assumed to be quintet and triplet states, respectively. According to the TD-DFT calculations, the Q excited state of 6cH-Im which is initially a pure π-π* state, crosses the Fe–CO dissociative state (2A') without large elongation of the Fe–CO bond. In contrast, the Q state of the 5cH does not cross the Fe–CO dissociative state but results in the formation of the excited spin state with a bent Fe–C–O. Consequently, photodisomarization from linear to bent Fe–C–O in the 5cH is a likely mechanism for apparent unphotodissociation.

X-F-10 Mechanism for Transduction of the Ligand-Binding Signal in Heme-Based Gas Sensory Proteins Revealed by Resonance Raman Spectroscopy

UCHIDA, Takeshi; KITAGAWA, Teizo

[*Acc. Chem. Res.* **38**, 662–670 (2005)]

Gene analysis has revealed a variety of new heme-containing gas sensory proteins in organisms ranging from bacteria to mammals. These proteins are composed of sensor, communication, and functional domains. The sensor domain contains a heme that binds effector molecules such as NO, O_2, or CO. Ligand binding by the sensor domain modulates the physiological role of the protein, such as DNA binding in the case of transcriptional factors or the catalytic reaction rate in the case of enzymes. This review summarizes resonance Raman (RR) studies, including static and time-resolved measurements, which have enabled elucidation of the mechanisms by which binding of specific target molecule by the sensor domain is transduced to alteration of the functional domain. These studies have shown that signals can be conveyed from the heme to the functional domain *via* three different pathways: i) a distal pathway, ii) a proximal pathway, and iii) a heme peripheral pathway.

X-F-11 UV Resonance Raman Study of Model Complexes of the Cu_B Site of Cytochrome *c* Oxidase

NAGANO, Yasutomo; LIU, Jin-Gang[1]; NARUTA, Yoshinori[1]; KITAGAWA, Teizo
([1]Kyushu Univ.)

[*J. Mol. Struct.* **735-736**, 279–291 (2005)]

A newly designed model complex for the Cu_B site of cytochrome *c* oxidase (CcO), that is, Cu coordinated by two free imidazoles and an imidazole covalently linked to *p*-cresol [Cu^{II}**BIAIP**Br]Br, (**BIAIP** = 2-[4-[[Bis(1-methyl-1*H*-imidazol-2-ylmethyl)amino]methyl]-1*H*-imidazol-1-yl]-4-methylphenol), and related molecules have been investigated with absorption and ultraviolet resonance Raman (UVRR) spectroscopy employing the excitation wavelengths between 220 and 290 nm. Attention was focused on the electron delocalization through the cross-linkage between the phenol and imidazole rings, and the influences by the coordination of Cu^{II} to imidazole. In addition to the ν_{8a} and ν_{8b} modes of *p*-cresol, a number of Raman bands involving vibrations of the imidazole moiety have been intensity-enhanced despite Raman excitation in resonance with the π-π* transition of phenol, indicating appreciable mixing of the π systems of imidazole and phenol rings. Furthermore, two kinds of imidazoles seem to be differential; one is the imidazole linked to *p*-cresol which yielded Raman bands at 1249, 1191, and 1141 cm^{-1} for protonated Cu^{II}-BIAIP, and the other is one not linked to *p*-cresol, which yielded an intense band at 1488 cm^{-1} band. Raman enhancement of the latter mode seems to be caused by preresonance to the lowest π-π* transition of imidazole *via* the A-term mechanism. The Raman excitation profile (REP) of ν_{8a} mode for the deprotonated phenol of the Cu^{II}-complex revealed a weak local maximum corresponding to the L_a band around 240 nm. Raman enhancement by the L_a band was relatively weaker for the Cu^{II}-complex than for the Zn^{II}-complex and metal-free ligand, suggesting the more extensive mixing of π systems of *p*-cresol-imidazole through the cross-linkage for the Cu^{II}-complex.

X-F-12 Resonance Raman Investigation on the Specific Sensing Mechanism of a Target Molecule by Gas Sensory Proteins

OHTA, Takehiro; KITAGAWA, Teizo

[*Inorg. Chem.* **44**, 758–769 (2005)]

Specific sensing of gas molecules such as CO, NO, and O_2 is a unique function of gas sensory hemoproteins, while hemoproteins carry out a wide variety of functions such as oxygen storage/transport, electron transfer, and catalysis as enzymes. It is important in the gas sensory proteins that the heme domain not only recognizes their target molecule, but also discriminates against other gases having similar molecular structures. Coordination of a target molecule to the heme is supposed to alter the protein conformation in the vicinity of heme, and the conformation change is propagated to the effector domain where substrate turnover, DNA binding, or interaction with a signal transduction protein will be performed in a way different from the case in binding of other gases. To understand the appearance of such a specificity, we focus our attention on the ligand-protein interactions in the distal side of heme here. Practically, the metal ligand vibrations as well as internal modes of ligand and heme are measured with resonance Raman spectroscopy for wild-type and some mutant proteins with full-length or limited sensory region. On the basis of such observations together with the knowledge currently available, we will discuss the mechanism of specific sensing of a diatomic molecule in gas sensory proteins.

X-F-13 Communication Pathway between Heme and Protein in Myoglobin

GAO, Ying[1]; EL-MASHTOLY, Samir F.; PAL, Biswajit; HAYASHI, Takashi[2]; HARADA, Katsuyoshi[3]; NAKAGAWA, Tomoyuki[3]; KITAGAWA, Teizo
([1]SOKENDAI; [2]IMS and Osaka Univ.; [3]Kyushu Univ.)

[*J. Am. Chem. Soc.* submitted]

We investigated the communication pathway between heme and protein with sperm whale myoglobin as a model. It is known that Trp7 and Tyr151 exhibit UVRR spectral changes upon ligand binding to heme, we monitored their UVRR spectral changes for three kinds of proteins in which the plausible pathway was removed (*i.e.*, *via* His93, propionate-6, or propionate-7). The UVRR results demonstrate that the absence of the H-bonds between propionate-7 and both Ser92 and His97 significantly perturbs the transduction of a structural change in heme to Trp7, but the cleavage of the Fe–His(93) covalent bond eliminates the communication to Tyr151. Thus the H-bonds between the propionate-7 and the F-helix regulate the conformational changes of the A helix, while the Fe–His bond is responsible for a change in the C-terminus but not for the A helix.

X-F-14 FT-IR Approaches on Amyloid Fibril Structure

HIRAMATSU, Hirotsugu; KITAGAWA, Teizo

[*Biochim. Biophys. Acta* in press]

This review treats recent achievements of Fourier-transform infrared absorption spectroscopy on protein science, especially on amyloid fibril structure. It includes the brief explanation of theoretical background, description of related techniques, and recent applications to analysis of fibril structure. Concerns to theoretical background, successful analysis of Amide I in terms of transition dipole coupling between the C=O oscillators in peptide main chain has been described. The theory enables us to estimate a content of secondary structure in a protein. Related experimental techniques such as linear dichroism measurement, application of microscope, and isotope labeling, are introduced. The linear-dichroism measurement brings direct information on molecular orientation, microscope enables to treat a well-prepared particle, and isotope-label technique allows our structural discussion with one-residue resolution. Application of IR absorption spectroscopy and related techniques on amyloid fibril structure is reviewed. The model obtained is compared with protein native structure.

X-F-15 Structural and Spectroscopic Characterization of (μ-Hydroxo or μ-Oxo)(μ-Peroxo)Diiron(III) Complexes: Models for Peroxo Intermediates of Non-Heme Dilron Proteins Structural and Spectroscopic Characterization of (μ-Hydroxo or μ-Oxo)(μ-Peroxo)Diiron(III) Complexes: Models for Peroxo Intermediates of Non-Heme Dilron Proteins

ZHANG, Xi[1]; FURUTACHI, Hideki[1]; FUJINAMI, Shuhei[1]; NAGATOMO, Shigenori; MAEDA, Yonezo[2]; WATANABE, Yoshihito[3]; KITAGAWA, Teizo; SUZUKI, Masatatsu[1]
([1]Kanazawa Univ.; [2]Kyushu Univ.; [3]IMS and Nagoya Univ.)

[*J. Am. Chem. Soc.* **127**, 826–827 (2005)]

(μ-Hydroxo or oxo)(μ-1,2-peroxo)diiron(III) complexes having a tetradentate tripodal ligand (L) containing a carboxylate sidearm $[Fe_2(\mu\text{-OH or }\mu\text{-O})(\mu\text{-}O_2)(L)_2]^{n+}$ were synthesized as models for peroxo-intermediates of non-heme diiron proteins and characterized by various physicochemical measurements including X-ray analysis, which provide fundamental structural and spectroscopic insights into the peroxodiiron(III) complexes.

X-F-16 Axial Ligand Substituted Nonheme Fe^{IV}=O complexes: Observation of Near-UV LMCT Bands and Fe=O Raman Vibrations

SASTRI, Chivukula V.[1]; PARK, Mi Joo[1]; OHTA, Takehiro; JACKSON, Timothy A.[2]; STUBNA,

Audria[3]; SEO, Mi Sook[1]; LEE, Jimin[1]; KIM, Jinheung[1]; KITAGAWA, Teizo; MUNCK, Eckard[3]; QUE, Lawrence Jr.[2]; NAM, Wonwoo[1]
([1]Ewha Womans Univ.; [2]Univ. Minnesota; [3]Carnegie Mellon Univ.)

[*J. Am. Chem. Soc.* **127**, 12494–12495 (2005)]

Axial ligand substitution of a mononuclear nonheme oxoiron(IV) complex, $[Fe^{IV}(O)(TMC)(NCCH_3)]^{2+}$ (**1**) (TMC = 1,4,8,11-tetramethyl-1,4,8,11-tetraazacyclotetradecane), leads to the formation of new Fe^{IV}=O species with relatively intense electronic absorption features in the near-UV region. The presence of these near-UV features allowed us to make the first observation of Fe=O vibrations of S = 1 mononuclear nonheme oxoiron(IV) complexes by resonance Raman spectroscopy. We have also demonstrated that the reactivity of nonheme oxoiron(IV) intermediates is markedly influenced by the axial ligands.

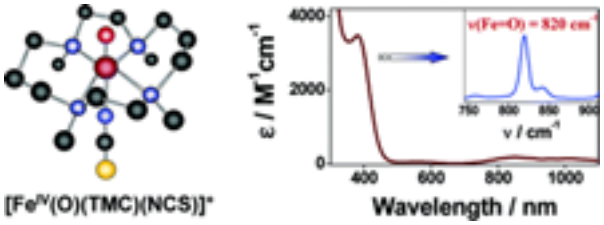

X-F-17 Reversible O–O Bond Cleavage and Formation of a Peroxo Moiety of a Peroxocarbonate Ligand Mediated by an Iron(III) Complex

FURUTACHI, Hideki[1]; HASHIMOTO, Koji[1]; NAGATOMO, Shigenori; ENDO, Taichi[1]; FUJINAMI, Shuhei[1]; WATANABE, Yoshihito[2]; KITAGAWA, Teizo; SUZUKI, Masatatsu[1]
([1]Kanazawa Univ.; [2]IMS and Nagoya Univ.)

[*J. Am. Chem. Soc.* **127**, 4550–4551 (2005)]

A mononuclear iron(III) complex containing a peroxocarbonate ligand, $[Fe(qn)_2(O_2C(O)O)]^-$ (qn = quinaldinate), underwent the reversible O–O bond cleavage and reformation of the peroxo group *via* the formation of Fe^{IV}=O or Fe^{V}=O species, which was confirmed by the resonance Raman and ESI-TOF/MS measurements.

X-F-18 Synthesis and Reactivity of a (μ-1,1-Hydroperoxo)(μ-Hydroxo)Dicopper(II) Complex: Ligand Hydroxylation by a Bridging Hydroperoxo Ligand

ITOH, Kyosuke[1]; HAYASHI, Hideo[1]; FURUTACHI, Hideki[1]; MATSUMOTO, Takahiro[1]; NAGATOMO, Shigenori; TOSHA, Takehiko; TERADA, Shoichi[1]; FUJINAMI, Shuhei[1]; SUZUKI, Masatatsu[1]; KITAGAWA, Teizo
([1]Kanazawa Univ.)

[*J. Am. Chem. Soc.* **127**, 5212–5223 (2005)]

A new tetradentate tripodal ligand (L3) containing sterically bulky imidazolyl groups was synthesized, where L3 is tris(1-methyl-2-phenyl-4-imidazolylmethyl) amine. Reaction of a bis(μ-hydroxo)dicopper(II) complex, $[Cu_2(L3)_2(OH)_2]^{2+}$ (**1**), with H_2O_2 in acetonitrile at –40 °C generated a (μ-1,1-hydroperoxo)dicopper(II) complex $[Cu_2(L3)_2(OOH)(OH)]^{2+}$ (**2**), which was characterized by various physicochemical measurements including X-ray crystallography. The crystal structure of **2** revealed that the complex cation has a Cu_2(μ-1,1-OOH)(μ-OH) core and each copper has a square pyramidal structure having an N_3O_2 donor set with a weak ligation of a tertiary amine nitrogen in the apex. Consequently, one pendant arm of L3 in **2** is free from coordination, which produces a hydrophobic cavity around the Cu_2(μ-1,1-OOH)(μ-OH) core. The hydrophobic cavity is preserved by hydrogen bondings between the hydroperoxide and the imidazole nitrogen of an uncoordinated pendant arm in one side and the hydroxide and the imidazole nitrogen of an uncoordinated pendant arm in the other side. The hydrophobic cavity significantly suppresses the H/D and $^{16}O/^{18}O$ exchange reactions in **2** compared to that in **1** and stabilizes the Cu_2(μ-1,1-OOH)(μ-OH) core against decomposition. Decomposition of **2** in acetonitrile at 0 °C proceeded mainly *via* disproportionation of the hydroperoxo ligand and reduction of **2** to $[Cu(L3)]^+$ by hydroperoxo ligand. In contrast, decomposition of a solid sample of **2** at 60 °C gave a complex having a hydroxylated ligand $[Cu_2(L3)(L3\text{-}OH)(OH)_2]^{2+}$ (**2**-(L3-OH)) as a main product, where L3-OH is an oxidized ligand in which one of the methylene groups of the pendant arms is hydroxylated. ESI-TOF/MS measurement showed that complex **2**-(L3-OH) is stable in acetonitrile at –40 °C, whereas warming **2**-(L3-OH) at room temperature resulted in the *N*-dealkylation from L3-OH to give an *N*-dealkylated ligand, bis(1-methyl-2-phenyl-4-imidazolylmethyl)-amine (L2) in ~80% yield based on **2**, and 1-methyl-2-phenyl-4-formylimidazole (Phim-CHO). Isotope labeling experiments confirmed that the oxygen atom in both L3-OH and Phim-CHO come from OOH. This aliphatic hydroxylation performed by **2** is in marked contrast to the arene hydroxylation reported for some (μ-1,1-hydroperoxo)dicopper(II) complexes with a xylyl linker.

X-F-19 Spectroscopic and Redox Properties of a CooA Homologue from *Carboxydothermus hydrogenoformans*

INAGAKI, Sayaka[1]; MASUDA, Chiaki[2]; AKAISHI, Tetsuhiro[2]; NAKAJIMA, Hiroshi[3]; YOSHIOKA, Shiro; OHTA, Takehiro; PAL, Biswajit; KITAGAWA, Teizo; AONO, Shigetoshi
([1]SOKENDAI; [2]JAIST; [3]IMS and JAIST)

[*J. Biol. Chem.* **280**, 3269–3274 (2005)]

CooA is a CO-sensing transcriptional activator that contains a b-type heme as the active site for sensing its physiological effector, CO. In this study, the spectroscopic and redox properties of a new CooA homologue from *Carboxydothermus hydrogenoformans* (Ch-CooA) were studied. Spectroscopic and mutagenesis studies revealed that His-82 and the N-terminal α-amino group

were the axial ligands of the Fe(III) and Fe(II) hemes in Ch-CooA and that the N-terminal α-amino group was replaced by CO upon CO binding. Two neutral ligands, His-82 and the N-terminal α-amino group, are coordinated to the Fe(III) heme in Ch-CooA, whereas two negatively charged ligands, a thiolate from Cys-75 and the nitrogen atom of the N-terminal Pro, are the axial ligands of the Fe(III) heme in Rr-CooA. The difference in the coordination structure of the Fe(III) heme resulted in a large positive shift of redox potentials of Ch-CooA compared with Rr-CooA. Comparing the properties of Ch-CooA and Rr-CooA demonstrates that the essential elements for CooA function will be: (i) the heme is six-coordinate in the Fe(III), Fe(II), and Fe(II)–CO forms; (ii) the N-terminal is coordinated to the heme as an axial ligand, and (iii) CO replaces the N-terminal bound to the heme upon CO binding.

X-F-20 Structural Diversities of Active Site in Clinical Azole-Bound Forms between Sterol 14α-Demethylases (CYP51s) from Human and *Mycobacterium tuberculosis*

MATSUURA, Koji[1]; YOSHIOKA, Shiro[2]; TOSHA, Takehiko; HORI, Hiroshi[3]; ISHIMORI, Koichiro[4]; KITAGAWA, Teizo; MORISHIMA, Isao[1]; KAGAWA, Norio[5]; WATERMAN, Michael R.[5]
([1]Kyoto Univ.; [2]IMS and Vandervilt Univ.; [3]Osaka Univ.; [4]IMS and Kyoto Univ.; [5]Vandervilt Univ.)

[*J. Biol. Chem.* **280**, 9088–9096 (2005)]

To gain insights into the molecular basis of the design for the selective azole anti-fungals, we compared the binding properties of azole-based inhibitors for cytochrome P450 sterol 14α-demethylase (CYP51) from human (HuCYP51) and *Mycobacterium tuberculosis* (MtCYP51). Spectroscopic titration of azoles to the CYP51s revealed that HuCYP51 has higher affinity for ketoconazole (KET), an azole derivative that has long lipophilic groups, than MtCYP51, but the affinity for fluconazole (FLU), which is a member of the anti-fungal armamentarium, was lower in HuCYP51. The affinity for 4-phenylimidazole (4-PhIm) to MtCYP51 was quite low compared with that to HuCYP51. In the resonance Raman spectra for HuCYP51, the FLU binding induced only minor spectral changes, whereas the prominent high frequency shift of the bending mode of the heme vinyl group was detected in the KET- or 4-PhIm-bound forms. On the other hand, the bending mode of the heme propionate group for the FLU-bound form of MtCYP51 was shifted to high frequency as found for the KET-bound form, but that for 4-PhIm was shifted to low frequency. The EPR spectra for 4-PhIm-bound MtCYP51 and FLU-bound HuCYP51 gave multiple g values, showing heterogeneous binding of the azoles, whereas the single g_x and g_z values were observed for other azole-bound forms. Together with the alignment of the amino acid sequence, these spectroscopic differences suggest that the region between the B' and C helices, particularly the hydrophobicity of the C helix, in CYP51s plays primary roles in determining strength of interactions with azoles; this differentiates the binding specificity of azoles to CYP51s.

X-F-21 Stopped-Flow Spectrophotometric and Resonance Raman Analyses of Aldoxime Dehydratase Involved in Carbon-Nitrogen Triple Bond Synthesis

OINUMA, Ken-Ichi[1]; KUMITA, Hideyuki[1]; OHTA, Takehiro; KONISHI, Kazunobu[1]; HASHIMOTO, Yoshiteru[1]; HIGASHIBATA, Hiroki[1]; KITAGAWA, Teizo; SHIRO, Yoshitsugu[2]; KOBAYASHI, Michihiko[1]
([1]Univ. Tsukuba; [2]RIKEN Harima Inst./SPring-8)

[*FEBS Lett.* **579**, 1394–1398 (2005)]

On stopped-flow analysis of aliphatic aldoxime dehydratase (OxdA), a novel hemoprotein, a spectrum derived from a reaction intermediate was detected on mixing ferrous OxdA with butyraldoxime; it gradually changed into that of ferrous OxdA with an isosbestic point at 421 nm. The spectral change on the addition of butyraldoxime to the ferrous H320A mutant showed the formation of a substrate-coordinated mutant, the absorption spectrum of which closely resembled that of the above intermediate. These observations and the resonance Raman investigation revealed that the substrate actually binds to the heme in OxdA, forming a hexacoordinate low-spin heme.

X-F-22 Synthesis, Characterization, and Thermal Stability of New Mononuclear Hydrogenperoxocopper(II) Complexes with N_3O-Type Tripodal Ligands Bearing Hydrogen-Bonding Interaction Sites

YAMAGUCHI, Syuhei[1]; KUMAGAI, Akinori[1]; NAGATOMO, Shigenori; KITAGAWA, Teizo; FUNAHASHI, Yasuhiro[2]; OZAWA, Tomohiro[1]; JITSUKAWA, Koichiro[1]; MASUDA, Hideki[2]
([1]Nagoya Inst. Tech.; [2]IMS and Nagoya Inst. Tech.)

[*Bull. Chem. Soc. Jpn.* **78**, 116–124 (2005)]

In order to understand the effect of an oxygen-containing ligand on the physico-chemical properties and reactivities of hydrogenperoxocopper complexes, new copper(II) complexes with the N_3O-type tripodal ligand bearing pivalamido groups, *N*,*N*-bis(6-pivalamido-2-pyridylmethyl)glycine (Hbpga), and *N*,*N*-bis(6-pivalamido-2-pyridylmethyl)-β-alanine (Hbpaa), have been designed and synthesized. Copper(II) complexes without any external ligand and those with a monodentate ligand, such as azido and chloro, have been prepared and characterized with the aid of electronic absorption and ESR spectroscopic, cyclic voltammetric, and X-ray structure analytical methods. The redox potential values of the Cu(II) complexes, when they were compared with the Cu(II) complex of bis(6-pivalamido-2-pyridylmethyl)(2-pyridylmethyl)amine (bppa), reported previously, shifted toward the negative side upon the introduction of a carboxylate group in the place of one pyridine of bppa. Reactions of [Cu(bpga)]ClO_4 (**1a**) and [Cu(bpaa)]PF_6 (**2a**) with hydrogen peroxide in the presence of triethylamine in both MeCN and MeOH solutions gave mononuclear copper(II) com-

plexes with hydrogenperoxide(1-), Cu–bpga–OOH (**1d**) and Cu–bpaa–OOH (**2d**) systems, respectively. The intense absorption bands, assignable to LMCT ($HOO^- \rightarrow$ Cu(II)) and d–d bands, and ESR and resonance Raman spectra have revealed that they form trigonal bipyramidal copper complexes with OOH^- in an end-on fashion. The thermal stabilities of **1d** and **2d** have also been studied by following the reduction rate of the LMCT bands at 283 K. Those of copper(II) complexes with hydrogenperoxide(1-) have been reduced in the order **1d** > **2d** >> $[Cu(bppa)(OOH)]^+$ (**3d**), all of which are rather stable compared with that of Cu(II)–tpa–OOH (tpa = tris(2-pyridylmethyl)amine). These findings indicate that the hydrogenperoxocopper(II) complexes are activated by introducing carboxylate coordination, although they are stabilized by hydrogen-bonding interactions.

X-F-23 Spectroscopic Characterization of the Isolated Heme-Bound PAS-B Domain of Neuronal PAS Domain Protein 2 (NPAS2) Associated with Circadian Rhythms

KOUDO, Ryoji[1]; KUROKAWA, Hirofumi[1]; SATO, Emiko[1]; IGARASHI, Jotaro[1]; UCHIDA, Takeshi; SAGAMI, Ikuko[2]; KITAGAWA, Teizo; SHIMIZU, Toru[1]
([1]Tohoku Univ.; [2]Kyoto Pref. Univ.)

[*FEBS J.* **272**, 4153–4162 (2005)]

Neuronal PAS domain protein 2 (NPAS2) is an important transcription factor associated with circadian rhythms. This protein forms a heterodimer with BM AL1, which binds to the E-box sequence to mediate circadian rhythm-regulated transcription. NPAS2 has two PAS domains with hemebinding sites in the N-terminal portion. In this study, we overexpressed wild-type and His mutants of the PAS-B domain (residues 241–416) of mouse NPAS2 and then purified and characterized the isolated homebound proteins. Optical absorption spectra of the wild-type protein showed that the Fe(III), Fe(II) and Fe(II)–CO complexes are 6-coordinated lowspin complexes. On the other hand, resonance Raman spectra indicated that both the Fe(III) and Fe(II) complexes contain mixtures of 5-coordinated high-spin and 6-coordinated low-spin complexes. Based on inverse correlation between ν_{Fe-CO} and ν_{C-O} of the resonance Raman spectra, it appeared that the axial ligand trans to CO of the heme-bound PAS-B is His. Six His mutants (His266Ala, His289Ala, His300Ala, His 302Ala, His329Ala, and His335Ala) were generated, and their optical absorption spectra were compared. The spectrum of the His335Ala mutant indicated that its Fe(III) complex is the 5-coordinated high-spin complex, whereas, like the wild-type, the complexes for the five other His mutants were 6-coordinated low-spin complexes. Thus, our results suggest that one of the axial ligands of Fe(III) in PAS-B is His335. Also, binding kinetics suggest that heme binding to the PAS-B domain of NPAS2 is relatively weak compared with that of sperm whale myoglobin.

X-F-24 Covalent Cofactor Attachment to Proteins: Cytochrome *c* Biogenesis

STEVENS, Julie M.[1]; UCHIDA, Takeshi; DALTROP, Oliver[1]; FERGUSON, Stuart J.[1]
([1]Univ. Oxford)

[*Biochem. Soc. Trans.* **33**, 792–795 (2005)]

Haem (Fe-protoporphyrin IX) is a cofactor found in a wide variety of proteins. It confers diverse functions, including electron transfer, the binding and sensing of gases, and many types of catalysis. The majority of cofactors are non-covalently attached to proteins. There are, however, some proteins in which the cofactor binds covalently and one of the major protein classes characterized by covalent cofactor attachment is the *c*-type cytochromes. The characteristic haem-binding mode of *c*-type cytochromes requires the formation of two covalent bonds between two cysteine residues in the protein and the two vinyl groups of haem. Haem attachment is a complex post-translational process that, in bacteria such as *Escherichia coli*, occurs in the periplasmic space and involves the participation of many proteins. Unexpectedly, it has been found that the haem chaperone CcmE (cytochrome *c* maturation), which is an essential intermediate in the process, also binds haem covalently before transferring the haem to apocytochromes. A single covalent bond is involved and occurs between a haem vinyl group and a histidine residue of CcmE. Several *in vitro* and *in vivo* studies have provided insight into the function of this protein and into the overall process of cytochrome *c* biogenesis.

X-F-25 Structure and Dioxygen-Reactivity of Copper(I) Complexes Supported by Bis(6-methylpyridin-2-yl-methyl)amine Tridentate Ligands

OSAKO, Takao[1]; TERADA, Shohei[2]; TOSHA, Takehiko; NAGATOMO, Shigenori; FURUTACHI, Hideki[2]; FUJINAMI, Shuhei[2]; KITAGAWA, Teizo; SUZUKI, Masatatsu[2]; ITO, Shinobu[1]
([1]Osaka City Univ.; [2]Kanazawa Univ.)

[*Dalton Trans.* in press]

Structure and dioxygen-reactivity of copper(I) complexes $\mathbf{2^R}$ supported by *N*,*N*-bis(6-methylpyridin-2-ly-methyl)amine tridentate ligands $L2^R$ [R (*N*-alkyl substituent) = $-CH_2Ph$ (Bn), $-CH_2CH_2Ph$ (Phe) and $-CH_2CHPh_2$ (PhePh)] have been examined in comparison with those of copper(I) complex $\mathbf{1^{Phe}}$ of *N*,*N*-bis[2-(pyridin-2-ly)ethyl]amine tridentate ligand $L1^{Phe}$ and copper(I) complex $\mathbf{3^{Phe}}$ of *N*,*N*-bis(pyridin-2-ly-methyl) amine tridentate ligand $L3^{Phe}$. Copper(I) complexes $\mathbf{2^{Phe}}$ and $\mathbf{2^{PhePh}}$ exhibit a distorted trigonal pyramidal structure involving a d-π interaction with an η^1-binding mode between the metal ion and one of the *ortho*-carbon atoms of the phenyl group of the ligand side arm [$-CH_2CH_2Ph$ (Phe) and $-CH_2CHPh_2$ (PhePh)]. Strength of the d-π interaction in $\mathbf{2^{Phe}}$ and $\mathbf{2^{PhePh}}$ is weaker than that of the d-π interaction with an η^2-binding mode in $\mathbf{1^{Phe}}$ but stronger than that of the η^1 d-π interaction in

$\mathbf{3}^{\mathbf{Phe}}$. Existence of a weak d-π interaction in $\mathbf{2}^{\mathbf{Bn}}$ in solution was also suggested, but its binding mode was not clear. Redox potential of copper(I) is also affected by the supporting ligand; $L3^{Phe}$ with the highest donor ability among the ligands gave the lowest $E_{1/2}$ value of the copper(I) complex, while $L1^{Phe}$ with the lowest donor ability showed the highest $E_{1/2}$ value. The redox potentials of 2^R were found between them, indicating that the electron-donor ability of $L2^R$ is between those of $L1^{Phe}$ and $L3^{Phe}$. This was reflected in the copper(I)-dioxygen reactivity, where the reaction rate of copper(I) complex toward O_2 dramatically increases in the order of $\mathbf{1}^{\mathbf{R}} < \mathbf{2}^{\mathbf{R}} < \mathbf{3}^{\mathbf{R}}$. Structure of the resulting Cu_2/O_2 intermediate was also altered by the supporting ligand. Oxygenation of copper(I) complex $\mathbf{2}^{\mathbf{R}}$ at a low temperature gave a (μ-η^2:η^2-peroxo)dicopper(II) complex as in the case of $\mathbf{1}^{\mathbf{Phe}}$, but its O–O bond is relatively weakened as compared to the peroxo complex derived from $\mathbf{1}^{\mathbf{Phe}}$, and a small amount of a bis(μ-oxo)dicopper(III) complex co-existed. These results can be attributed to the higher electron-donor ability of $L2^R$ as compared to $L1^{Phe}$. On the other hand, the fact that $\mathbf{3}^{\mathbf{Phe}}$ mainly afforded a bis(μ-oxo)dicopper(III) complex suggests that the electron-donor ability of $L2^R$ is not high enough to support the higher oxidation sate of copper(III) of the bis(μ-oxo) complex.

X-F-26 Resonance Raman and FT-IR Studies on Proximal and Distal Histidine Environment of Cytoglobin and Neuroglobin

SAWAI, Hitomi[1]; MAKINO, Masatomo[1]; MIZUTANI, Yasuhisa[2]; OHTA, Takehiro; SUGIMOTO, Hiroshi[3]; UNO, Tadayuki[4]; KAWADA, Norifumi[1]; YOSHIZATO, Katsutoshi[1]; KITAGAWA, Teizo; SHIRO, Yoshitsugu[3]
([1]Univ. Hyogo; [2]IMS and Kobe Univ.; [3]RIKEN Harima Inst./SPring8; [4]Osaka Univ.)

[*Biochemistry* in press]

Cytoglobin (Cgb) and neuroglobin (Ngb) are first examples of hexa-coordinated globins of humans and other vertebrates, where a histidine (His) residue is an endogenous ligand at the sixth position of the heme iron in both the ferric and the ferrous forms. The static and time-resolved resonance Raman and FT-IR spectroscopic techniques were applied to examine the structures in the heme environment of these globins. Using the picosecond time-resolved resonance Raman (ps-TR[3]) spectroscopy, the Fe–His stretching (ν_{Fe-His}) bands of transient five-coordinate heme species for Cgb and Ngb, yielded upon photolysis of the carbon monoxide (CO) adducts, were observed at 229 and 221 cm^{-1}, respectively. The ν_{Fe-His} band of Cgb and Ngb did not exhibit any time-dependent shift in the 20–1000 ps time domain, being contrasted to the case of Mb. In combination of the present spectroscopic data with the crystallographic ones reported so far, it was likely suggested that the structure of Cgb and Ngb in the heme pocket would be altered upon the CO binding, and the altered structures are different from that of Mb, but the scales of the structural alteration are different between Cgb and Ngb. To investigate the structural property of the heme distal side for the ligand-bound forms, the sets of (ν_{Fe-CO}, ν_{C-O}, δ_{Fe-C-O}) and (ν_{Fe-NO}, ν_{N-O}, δ_{Fe-N-O}) for the CO and NO complexes of Cgb and Ngb were observed. On the basis of the spectral comparison of some distal mutants for Cgb (H81A, H81V, R84A, R84K, R84T) and Ngb (H64A, H64V, K67A, K67R, K67T), it was found that three conformers were present in their CO complexes, and the distal His (His81 in Cgb and His64 in Ngb), which were replaced by the exogenous CO ligand, mainly contributes to the inter-conversion of the conformers. These structural characteristics of Cgb and Ngb were discussed in relation to their ligand binding and physiological properties.

X-F-27 Dynamic Ligation Properties of the *Escherichia coli* Heme Chaperone CcmE to Non-Covalently Bound Heme

STEVENS, Julie M.[1]; UCHIDA, Takeshi; DALTROP, Oliver[1]; KITAGAWA, Teizo; FERGUSON, Stuart J.[1]
([1]Univ. Oxford)

[*J. Biol. Chem.* submitted]

The cytochrome *c* maturation protein CcmE is an essential membrane-anchored heme chaperone involved in the post-translational covalent attachment of heme to *c*-type cytochromes in Gram-negative bacteria such as *Escherichia coli*. Previous *in vitro* studies have shown that CcmE can bind heme both covalently (*via* a histidine residue) and non-covalently. In this work we present results on the latter form of heme binding to a soluble form of CcmE. Examination of a number of site-directed mutants of *E. coli* CcmE by resonance Raman spectroscopy has identified ligands of the heme iron and provided insight into the initial steps of heme binding by CcmE before it binds the heme covalently. The heme-binding histidine (H130) appears to ligate the heme iron in the ferric oxidation state but two other residues ligate the iron in the ferrous form, thereby freeing H130 to undergo covalent attachment to a heme vinyl group. It appears that the heme ligation in the non-covalent form is different from that in the holo-form, suggesting that a change in ligation could act as a trigger for the formation of the covalent bond.

X-G Collaborative Research with FANTOM Consortium

The collaboration with Okazaki Institute for Integrative Bioscience has focused with the interaction of the Fantom Consortium. In this context, the group of Dr. Seto has focused on the analysis of the Ubiquitin protein within the Fantom-3 dataset, and to analyze the function.

X-G-1 The international Consortium, FANTOM*, Discovered UBL Domains Interspersed over Mammalian Genomes

HAYASHIZAKI, Yoshihide
(IMS and RIKEN GSC)

Ubiquitin is a protein that has been well investigated in the fields of protein degradation and transport systems. Several proteins are reported that they have ubiquitin-like sequence, UBL domains. These proteins were named UBL-containing proteins, and comparative analyses of all UBL-containing proteins were performed among various species, including humans, mice, flies, worms, and yeast in this report.

We compared human UBL-containing proteins with mouse UBL-containing proteins, and found 43 orthologous pairs (74% in human UBL-containing proteins). The UBL-containing proteins were divergent protein family. We found two human UBL-containing proteins whose mouse orthologs did not possess a UBL domain. We also found three mouse UBL-containing proteins whose human orthologs did not possess a UBL domain. Moreover, 12 human UBL-containing proteins had no orthologs in the mouse genome, and 8 mouse UBL-containing proteins had no human orthologs. About 60% of the conserved UBL-containing proteins between human and mouse were expressed in the nervous system in FANTOM3 dataset. By using the phylogenic analysis of all UBL domains in humans, mice, flies, worms, and yeast, we found that 33% of UBL domains were species-specific, and that 40% of UBL domains were found in the human/mouse conserved group. Therefore, this study on the UBL-containing proteins show a tendency to diversify their amino acid sequences during the evolution.

* FANTOM: Functional Annotation Of Mouse